Synthesis and Structure−Activity Relationships of Suramin-Derived $P2Y_{11}$ Receptor Antagonists with Nanomolar Potency

Heiko Ullmann,[†] Sabine Meis,[†] Darunee Hongwiset,[†] Claudia Marzian,[†] Michael Wiese,[†] Peter Nickel,[†] Didier Communi,[‡] Jean-Marie Boeynaems,[‡] Christian Wolf,[§] Ralf Hausmann,[§] Günther Schmalzing,[§] and Matthias U. Kassack*,[†]

Pharmaceutical Institute, University of Bonn, An der Immenburg 4, D-53121 Bonn, Germany, Institute of Interdisciplinary Research, School of Medicine, Université Libre de Bruxelles, 808 Route de Lennik, 1070 Brussels, Belgium, and Department of Molecular Pharmacology, RWTH Aachen University, Wendlingweg 2, D-52074 Aachen, Germany

Received April 4, 2005

Selective and potent $P2Y_{11}$ receptor antagonists have yet to be developed, thus impeding an evaluation of this G protein-coupled receptor mainly expressed on immune cells. Taking suramin with moderate inhibitory potency as a template, 18 ureas with variations of the methyl groups of suramin and their precursors were functionally tested at $P2Y_{11}$, $P2Y_1$, and $P2Y_2$ receptors. Fluorine substitution of the methyl groups of suramin led to the first nanomolar $P2Y_{11}$ antagonist (**8f**, NF157, pK_i: 7.35). For selectivity, **8f** was also tested at various P2X receptors. **8f** displayed selectivity for $P2Y_{11}$ over $P2Y_1$ (>650-fold), $P2Y_2$ (>650-fold), $P2X_2$ (3-fold), $P2X_3$ (8-fold), $P2X_4$ (>22-fold), and $P2X_7$ (>67-fold) but no selectivity over $P2X_1$. QSAR studies confirm that residues with favored resonance and size parameters in the aromatic linker region can indeed lead to an increased potency as is the case for **8f**. A symmetric structure linking two anionic clusters seems to be required for bioactivity. **8f** may be helpful for studies evaluating the physiological role of $P2Y_{11}$ receptors.

Introduction

Purine receptors comprise the P1 (adenosine) and P2 (nucleotide) receptors.[1] P2 receptors are further divided into two subfamilies: ionotropic P2X ($P2X_{1-7}$) and metabotropic (G protein-coupled) P2Y receptors ($P2Y_{1,2,4,6,11-14}$).[2−5] P2X and P2Y receptors are widely expressed and thus involved in diverse physiological functions.[6] From a medicinal chemist's point of view, little work has been done so far on $P2Y_{11}$ receptors. $P2Y_{11}$ receptors seem to be involved in the maturation of neutrophils and dendritic cells and seem to play a role in controlling cardiomyocyte contractility.[7−9] However, no selective and potent inhibitors of $P2Y_{11}$ receptors are currently available, thus hampering the determination of their physiological role. Only suramin (Figure 1), a polysulfonated naphthylurea, is described as a $P2Y_{11}$ antagonist and showed modest selectivity for $P2Y_{11}$ over other P2Y but not P2X receptors.[10−12] Suramin served as a highly successful chemical lead for the development of potent and selective P2X antagonists in our group.[13−17] The purpose of this study was to again use suramin as a template for developing potent $P2Y_{11}$ receptor antagonists with selectivity for $P2Y_{11}$ over other P2Y and P2X receptors. Thus, a series of suramin analogues with variations of the methyl groups of suramin[18] was augmented by three additional substitutions of the methyl groups and subsequently, 53 compounds (ureas and precursors) were pharmacologically evaluated at recombinant $P2Y_{11}$ receptors. A quantitative structure−activity analysis of the suramin-type ureas containing only variations of the methyl group of suramin was performed. The selectivity for $P2Y_{11}$ over other P2Y receptors was estimated at $P2Y_1$ and $P2Y_2$, representing two main P2Y subtypes that are activated either by adenine nucleotides ($P2Y_1$) or uracil nucleotides (UTP, UDP: $P2Y_2$).[4,12] Further, the most potent compound **8f** was also tested at various P2X receptors.

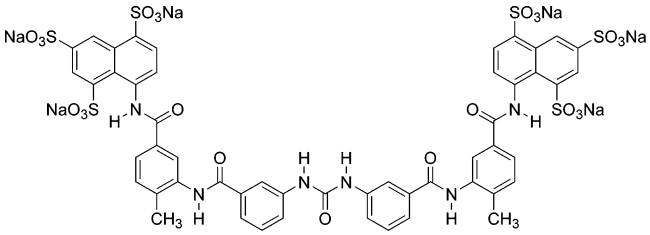

Figure 1. Structural formula of suramin.

Chemistry

Taking suramin (**8b**, Figure 1) as the chemical lead, compounds with a replacement of the methyl groups of suramin by chlorine, methoxy, and methoxymethyl substituents were synthesized (**8g**−**i**, Scheme 1). The other suramin analogues **8a**,**c**−**f** were prepared for biological evaluation as reported in the literature.[18] Since no analytical data (especially no NMR data) have been provided in these earlier studies aimed at the development of potential filaricides,[18] besides the synthesis of new compounds (**8g**−**i**), analytical data proving the identity and purity of all compounds (ureas and precursors) are presented in this paper. 4-(Bromomethyl)benzoic acid was used to synthesize 4-methoxymethylbenzoic acid according to Olson, and Harwood et al., which was subsequently nitrated to 4-(methoxymethyl)-3-nitrobenzoic acid by a standard nitration procedure.[19−21]

* To whom correspondence should be addressed. Tel: +49-228-735240. Fax: +49-228-737929. E-mail: kassack@uni-bonn.de.
[†] University of Bonn.
[‡] Université Libre de Bruxelles.
[§] RWTH Aachen University.

10.1021/jm050301p CCC: $30.25
Published on Web 10/01/2005

Scheme 1. Syntheses of the Ureas **5a**−**i** and **8a**−**i**[a]

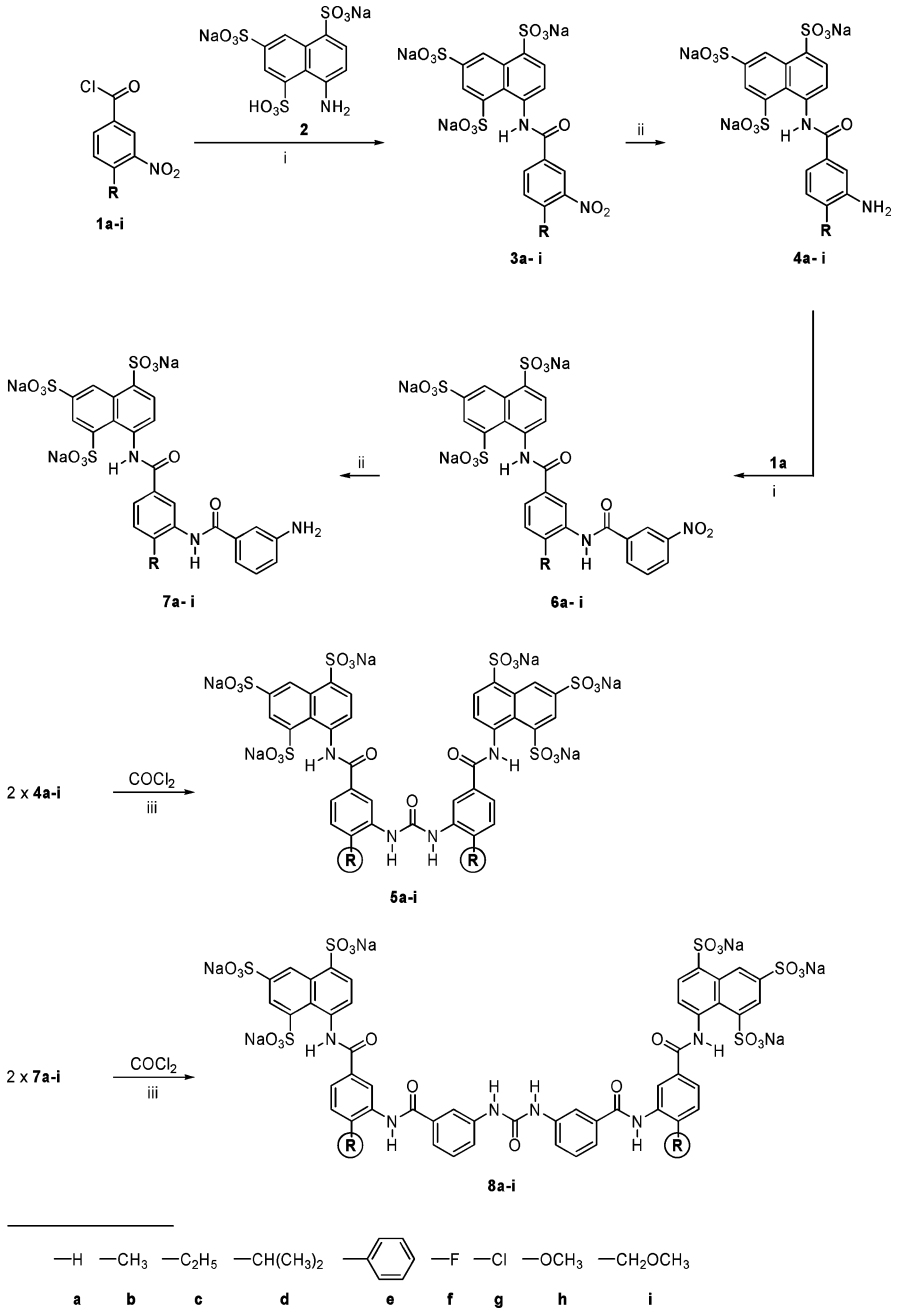

[a] Syntheses of ureas **5b**−**f** and **8a**−**f** were reported by Nickel et al., synthesis of **5a** by Kassack et al.[16,18] Reaction conditions for the syntheses of **5g**−**i** and **8g**−**i**: (i) **2** in water, pH 4, **1a**,**g**−**i** in toluene, rt, 6 h, 94.2% (**3g**), 89.9% (**3h**), 88.3% (**3i**), 22.9% (**6g**), 92.6% (**6h**), 92.5% (**6i**). (ii) **4h,i**, **7h,i**: Pd (10%) on charcoal, H_2O, 4 bar H_2, rt, overnight, 90.6% (**4h**), 91.6% (**4i**), 90.2% (**7h**), 86.4% (**7i**); **4g**, **7g**: H_2O, $FeCl_2 \cdot 4H_2O$, pH 7.5, 6 h, 88.9% (**4g**), 76.3% (**7g**). (iii) **4g**−**i**, **7g**−**i** in H_2O, pH 4, phosgene (20%) in toluene, rt, 6 h, 80.7% (**5g**), 56.9% (**5h**), 75.6% (**5i**), 76.4% (**8g**), 89.2% (**8h**), 88.8% (**8i**).

The nitrobenzoyl chlorides **1g**−**i** were synthesized according to Gattermann and Wieland, and Henecka.[22,23] Synthesis of the amide bonds resulting in the carboxamides **3g**−**i** and **6g**−**i**, the reduction of nitro to amino groups (**4h**,**i** and **7h**,**i**), and the synthesis of the ureas **5g**−**i** and **8g**−**i** by use of a solution of phosgene in toluene were all performed according to Kassack et al. (Scheme 1).[16] Compounds **4g** and **7g** (reduction of 4-chloro-3-nitrobenzoic acid derivatives to the corresponding amino compounds) were synthesized according to Muth and Sauerbier (Scheme 1).[24] The identity of the compounds was confirmed by nuclear magnetic resonance (NMR, ^{1}H, ^{13}C: only for the most potent compound **8f** and its **f**-series precursors **3f**−**7f**) and IR spectroscopy. Protons and carbons were attributed to their corresponding ^{1}H and ^{13}C signals, on the basis of spectra recorded and published for other suramin analogues.[16,25] In addition, electron spray (ES) mass spectrometry was performed for the bioactive ureas **8a**,**c**−**i**. Since all synthesized compounds were obtained as sodium salts, ES mass spectra were monitored in a 2 mM solution of ammonium acetate yielding various anions (1−5 negative charges) with up to five sodium ions. Purity of the compounds was checked by elemental analysis (C, H, N), thin-layer chromatography (TLC), and a high-performance liquid chromatography method formerly published.[26] HPLC and TLC purity was >95% for all compounds.

Biological Results

Target compounds (ureas **5a**−**i** and **8a**−**i**) as well as their precursors (nitro and amino derivatives **3**, **4**, **6**, **7a**−**i**) were tested for interaction with $P2Y_{11}$ receptors recombinantly expressed in 1321N1 astrocytoma cells[10,27] and at human embryonic kidney (HEK293) cells endogenously expressing $P2Y_1$ and $P2Y_2$ receptors as has been shown by Schachter et al. and Yu et al.[28,29] The expression of $P2Y_1$ and $P2Y_2$ receptors in our HEK293 cells was confirmed by RT-PCR using $P2Y_1$ and $P2Y_2$ specific primer pairs and yielded cDNA fragments with an expected size of 247 bp for $P2Y_2$ (Figure 2a, lane 2) and 389 bp for $P2Y_1$ (Figure 2a, lane 3) as shown by agarose gel electrophoresis. Interaction of test compounds with P2Y receptors was analyzed by using a fluorescence calcium assay described by Kassack et al.[30] Functional activation of P2Y receptors by agonist stimulation leads to an increase in cytosolic Ca^{2+} concentration at $P2Y_1$, $P2Y_2$, and $P2Y_{11}$ receptors (Figure 2b−d). The use of HEK293 cells for interaction analysis of compounds with $P2Y_1$ and $P2Y_2$ receptors is based on the selectivity of the respective agonists. 2-MeSADP is more than 15 000-fold selective for $P2Y_1$ over $P2Y_2$ receptors, and UTP is more than 500-fold selective for $P2Y_2$ over $P2Y_1$ receptors.[6,12] Figure 2b shows a concentration−response curve of 2-MeSADP and an inhibition curve of PPADS using 31.6 nM 2-MeSADP for receptor stimulation at $P2Y_1$ receptors. Figure 2c shows a concentration−response curve of UTP and an inhibition curve of suramin (**8b**) using 3.16 μM UTP as agonist at $P2Y_2$ receptors. $P2Y_{11}$ receptors were stimulated by ATPγS. No signal was observed upon addition of ATPγS or ATP to 1321N1 wild-type cells (data not shown), thus showing the selectivity of the test system for $P2Y_{11}$ receptors. Figure 2d displays a concentration−response curve of ATPγS and the slightly less potent ATP at recombinant $P2Y_{11}$ receptors. Test compounds were screened for agonist and antagonist effects at the three examined P2Y receptors.

None of the synthesized compounds (precursors or ureas) showed any agonist effects at $P2Y_1$, $P2Y_2$, or $P2Y_{11}$ receptors up to a concentration of 100 μM (data not shown). All nitro and amino precursors of the ureas **5a**−**i** and **8a**−**i** showed less than 40% inhibition up to 100 μM at each of the three tested P2Y receptors, respectively (data not shown). The inhibitory potency at $P2Y_1$, $P2Y_2$, and $P2Y_{11}$ receptors of the symmetric ureas **5a**−**i** and **8a**−**i** expressed as % inhibition at a concentration of 100 μM is given in Table 1. Only compounds **5f**,**g** and **8a**,**b**,**e**,**f** blocked $P2Y_1$ receptors with more than 50% at 100 μM (54−75%, Table 1) but showed no effect if the concentration was reduced to 10 μM (data not shown). Similarly at $P2Y_2$ receptors, only **5h** and **8b**,**e**,**g** showed a weak antagonist activity at 100 μM (inhibition 50−73%, Table 1) and no inhibitory activity (inhibition < 20%) at a concentration of 10 μM (data not shown). Thus, all compounds have IC_{50} values at $P2Y_1$ and $P2Y_2$ receptors of >10 μM, and most compounds even >100 μM.

At $P2Y_{11}$ receptors, except for **5c**,**d**,**e**,**h**,**i** all urea derivatives blocked the agonist signal more than 50%, most large ureas (**8b**,**f**,**g**,**h**) even more than 90% at a concentration of 100 μM. For all compounds showing a % inhibition of >70, complete concentration−response

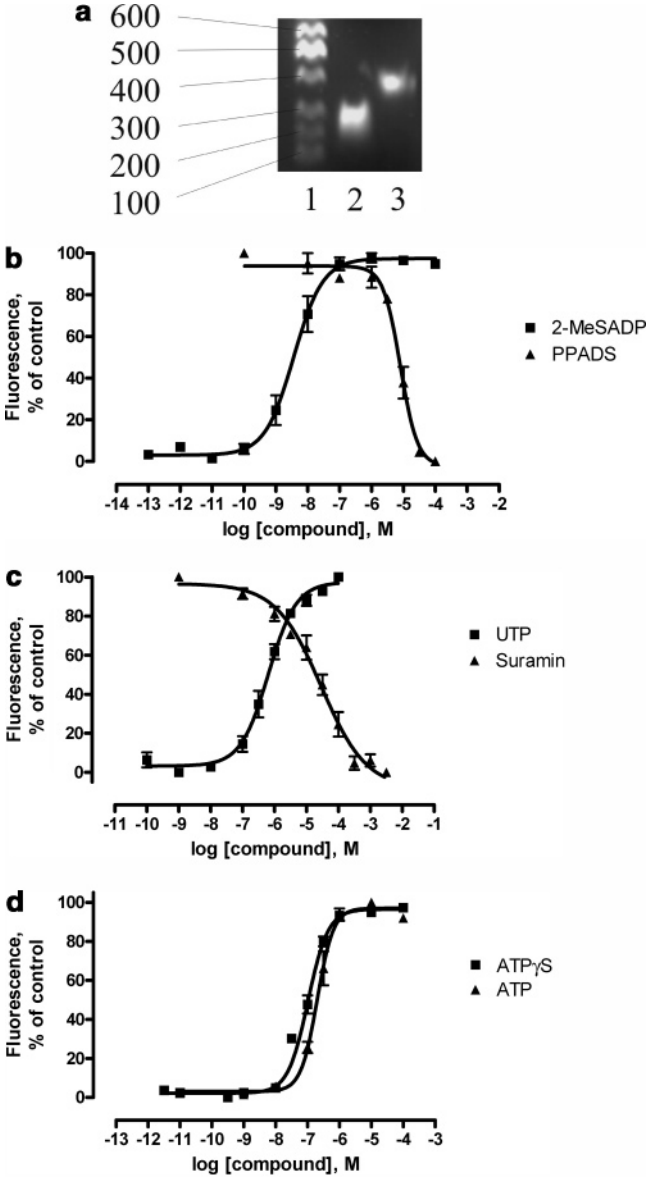

Figure 2. (a) Agarose gel electrophoresis of PCR-amplified $P2Y_1$ and $P2Y_2$ receptor fragments from native HEK293 cells. Lane 1: 100bp DNA-ladder (Fermentas, St. Leon-Rot, Germany); lane 2: $P2Y_2$ (247bp); lane 3: $P2Y_1$ (389bp). Detection of DNA-fragments was performed with SYBR Green (Bio-Rad, München, Germany). (b) Concentration−response curve of 2-MeSADP at $P2Y_1$ receptors in native HEK293 cells and concentration-dependent inhibition by PPADS of a response induced by 31.6 nM 2-MeSADP. Data shown are mean ± SEM of the pooled data of n independent experiments each with three replicates. pEC_{50} [2-MeSADP] = 8.44 ± 0.09, n = 4; pIC_{50} [PPADS] = 5.09 ± 0.06, n = 3. Hill coefficients were not significantly different from unity. (c) Concentration−response curve of UTP at $P2Y_2$ receptors in native HEK293 cells and concentration-dependent inhibition by suramin of a response induced by 3.16 μM UTP. Data shown are mean ± SEM of the pooled data of n independent experiments each with three replicates. pEC_{50} [UTP] = 6.19 ± 0.06, n = 6; pIC_{50} [suramin] = 4.54 ± 0.15, n = 4. Hill coefficients were not significantly different from unity. (d) Concentration−response curves of ATP and ATPγS at $P2Y_{11}$ receptors recombinantly expressed in 1321N1 cells. Data shown are mean ± SEM of the pooled data of n independent experiments each with three replicates. pEC_{50} [ATP] = 6.76 ± 0.07, n = 4. pEC_{50} [ATPγS] = 6.98 ± 0.03, n = 13. Hill coefficients were not significantly different from unity.

Table 1. Percent Inhibition by a Single Dose (100 μM) of Ureas **5a**−**i** and **8a**,**c**−**i**, and Suramin (**8b**) of Agonist-Induced Calcium Mobilization at Native P2Y$_1$ and P2Y$_2$ Receptors in HEK293 Cells and at P2Y$_{11}$ Receptors Recombinantly Expressed in 1321N1 Astrocytoma Cells[a]

compound	P2Y$_1$	P2Y$_2$	P2Y$_{11}$
5a	19.7 ± 10.5	24.0 ± 3.9	54.2 ± 1.0
5b	0 ± 4.2	28.4 ± 2.5	86.6 ± 1.7
5c	38.4 ± 9.6	20.8 ± 0.3	39.9 ± 1.8
5d	28.7 ± 1.0	14.2 ± 1.0	23.2 ± 5.4
5e	34.2 ± 2.5	0 ± 7.9	35.9 ± 0.9
5f	60.0 ± 5.7	0 ± 7.5	64.7 ± 1.8
5g	57.8 ± 4.0	0 ± 10.5	59.0 ± 1.8
5h	40.0 ± 5.0	53.6 ± 2.7	11.2 ± 1.9
5i	31.7 ± 6.1	13.0 ± 2.5	23.8 ± 1.8
8a	59.3 ± 9.0	31.6 ± 14.6	89.5 ± 1.2
8b, suramin	54.5 ± 10.3	50.5 ± 13.9	93.7 ± 0.8
8c	48.7 ± 10.9	48.8 ± 8.0	84.9 ± 3.1
8d	45.0 ± 9.8	31.1 ± 18.2	83.1 ± 1.1
8e	75.1 ± 5.1	73.2 ± 9.6	79.9 ± 1.1
8f	63.3 ± 15.5	42.8 ± 10.3	96.6 ± 2.9
8g	40.6 ± 24.2	55.2 ± 9.5	93.0 ± 1.2
8h	23.2 ± 29.4	44.9 ± 9.4	92.2 ± 1.2
8i	47.5 ± 7.4	44.3 ± 6.5	71.6 ± 3.0

[a] Data shown are mean ± SEM, $n \geq 3$.

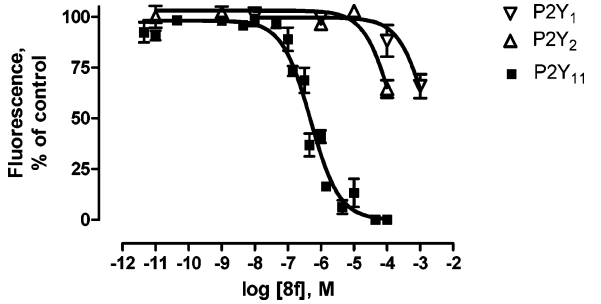

Figure 3. Concentration-dependent inhibition by **8f** of a response induced by injection of agonist at P2Y$_1$, P2Y$_2$, and P2Y$_{11}$ receptors, respectively. Data shown are mean ± SEM of the pooled data of three (P2Y$_{1,\ 2}$) or seven independent experiments each with three replicates. pIC$_{50}$ [P2Y$_1$] = 2.74 ± 0.12; pIC$_{50}$ [P2Y$_2$] = 3.77 ± 0.07; pIC$_{50}$ [P2Y$_{11}$] = 6.34 ± 0.06. Hill coefficients were not significantly different from unity.

curves were monitored. Figure 3 displays the concentration−response curves at P2Y$_1$, P2Y$_2$, and P2Y$_{11}$ receptors for the most potent compound **8f** containing normalized data from seven (P2Y$_{11}$) or three (P2Y$_{1,\ 2}$) independent experiments. IC$_{50}$ values were calculated as follows: P2Y$_{11}$: 463 ± 59 nM (corresponding to an apparent functional K_i value of 44.3 nM); P2Y$_1$: 1811 ± 312 μM (corresponding to an apparent functional K_i value of 187 μM); P2Y$_2$: 170 ± 17 μM (corresponding to an apparent functional K_i value of 28.9 μM). Table 2 lists apparent functional pK_i values of **5b** and all large ureas **8a**−**i** as well as their relative potencies referred to the most potent, fluorine-substituted compound **8f** which was set as 100%. Except for the small urea **5b** and the large ureas **8c** (R = ethyl) and **8i** (R = methoxymethyl), all other large ureas including suramin displayed pK_i values > 6, leaving their potency in the sub-micromolar range. Five out of nine large ureas demonstrate an equal or better inhibitory potency than suramin (**8b**). Among these are the hydrogen **8a**, the phenyl **8e**, the halogens (fluorine **8f**, chlorine **8g**), and the methoxy **8h** derivatives. The most potent P2Y$_{11}$ antagonist **8f** is ~ 7-fold more potent than suramin (**8b**). Furthermore, **8f** is at least 650-fold selective for P2Y$_{11}$ over P2Y$_1$ and P2Y$_2$ receptors (Figure 3). **8f** was also tested for interaction with different rat (r) and human (h) P2X receptors recombinantly expressed in *Xenopus laevis* oocytes. The effect of **8f** on rP2X$_1$, rP2X$_2$, rP2X$_3$, rP2X$_4$, rP2X$_7$, hP2X$_1$, hP2X$_3$, and hP2X$_4$ receptor-mediated currents was analyzed by using two-electrode voltage-clamp electrophysiology as described before.[17] Table 3 shows the potencies of **8f** at recombinant wild-type rat and human P2X receptors. As explained in the Experimental Section (Electrophysiological evaluation of **8f** at recombinant P2X receptors), IC$_{50}$ values at P2X receptors are close to or equal to K_i values. Thus, **8f** shows a similar potency for P2Y$_{11}$ and P2X$_1$ receptors. However, **8f** shows a small to medium selectivity for P2Y$_{11}$ over P2X$_2$ (3-fold) and P2X$_3$ (8-fold), and **8f** is very selective for P2Y$_{11}$ over P2X$_4$ (>22-fold) and P2X$_7$ (>67-fold) (calculated from the data in Tables 2 and 3).

Table 2. Apparent Functional pK_i ± SEM Values of **5b** and the Large Ureas **8a**,**c**−**i** and Suramin at P2Y$_{11}$ Receptors Recombinantly Expressed in 1321N1 Astrocytoma Cells[a]

compound	n	pK_i ± SE	relative potency
5b	3	5.12 ± 0.13	0.6
8a	3	6.95 ± 0.14	40
8b, suramin	6	6.52 ± 0.13	15
8c	3	6.00 ± 0.12	4.5
8d	4	6.35 ± 0.16	10
8e	3	6.52 ± 0.17	15
8f	7	7.35 ± 0.06	100
8 g	5	6.97 ± 0.06	42
8h	4	7.12 ± 0.04	59
8i	4	5.62 ± 0.08	1.9

[a] n: number of experiments. Relative potencies are normalized to the potency of **8f** which was set as 100.

Table 3. Potencies of **8f** at Wild Type P2X Receptors Recombinantly Expressed in *Xenopus laevis* Oocytes (pIC$_{50}$ ± SEM Values, $n \geq 3$)

P2X receptor	pIC$_{50}$
rP2X$_1$	7.09 ± 0.09
rP2X$_2$	6.86 ± 0.06
rP2X$_3$	6.11 ± 0.12
hP2X$_1$	7.20 ± 0.08
hP2X$_3$	6.45 ± 0.05
rP2X$_4$, hP2X$_4$	< 6
rP2X$_7$	< 5.5

Figure 3 displays a concentration−response curve of **8f** with a Hill coefficient not significantly different from unity, thus assuming a competitive behavior of **8f** at the orthosteric binding site of the P2Y$_{11}$ receptor. To further prove the competitiveness of **8f** and ATPγS, agonist (= ATPγS) concentration−response curves were monitored in the absence and presence of increasing concentrations of **8f**. Figure 4a shows the rightward shift of the concentration−response curves in the presence of **8f**. A Schild analysis of these data is displayed in Figure 4b and shows a straight line with a slope not significantly different from unity (slope: 0.851 ± 0.076; 95% confidence interval: 0.680 to 1.023). Thus, a competitive mechanism of **8f** can be assumed. The pA$_2$ value was estimated as 7.77 ± 0.18 (average ± SEM, n = 3). The pA$_2$ of **8f** is in a similar range as the pK_i (7.35, Table 2).

The homologous series of large ureas **8a**−**i** displayed a maximum 53-fold difference between the weakest (**8i**) and most potent compound (**8f**, Table 2). To identify molecular properties influencing the potency, a Hansch-

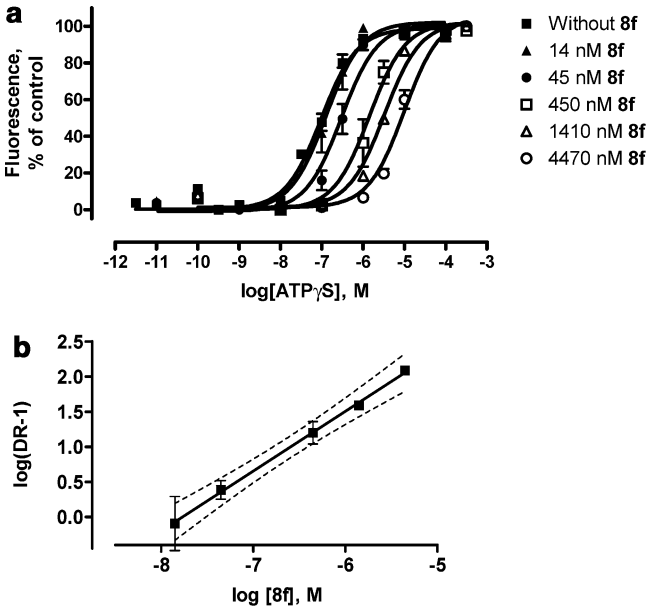

Figure 4. (a) Concentration−response curves for the effect of ATPγS on intracellular [Ca^{2+}] at $P2Y_{11}$ receptors recombinantly expressed in 1321N1 cells. ATPγS was tested alone as well as in the presence of increasing concentrations of **8f**. Data shown are representative for a typical experiment out of three each with 3−4 replicates. Hill coefficients are not significantly different from unity. (b) Functional analysis of the antagonist effect of **8f** at $P2Y_{11}$ receptors recombinantly expressed in 1321N1 cells (Schild plot analysis). The analysis was carried out by measuring the attenuation by **8f** of the ATPγS-induced increase in intracellular [Ca^{2+}]. Dashed lines show 95% confidence interval. Data points presented are mean ± SEM from three experiments each performed with 3−4 replicates. pA_2 was estimated as 7.77 ± 0.18 (mean ± SEM). Slope is not significantly different from unity.

type QSAR analysis correlating pK_i values of the large ureas **8a**−**i** with physicochemical parameters was performed. In addition to fragment constant descriptors, partial charges of atoms of the amide group in ortho-position of the residue R were calculated with quantum chemistry methods. Since molecular variations of the large ureas **8a**−**i** were only introduced into one position (residue R in Scheme 1), only one-half of the symmetric molecule was examined and the naphthalene sulfonic acid residues were abandoned for calculations. Best correlations between calculated and observed pK_i values were then obtained with the parameters for resonance (R), size (B5), and partial charge of the amide group oxygen in ortho-position of the variable residue R ($Q(O_{ortho})$). These parameters are listed in Table 4. Results of the correlation analyses are depicted in Figure 5. Regression with resonance (R) and size (B5) and regression with size (B5) and partial charge $Q(O_{ortho})$ yielded correlations of calculated and observed pK_i values with a r^2 of 0.880 and 0.851, respectively (Figure 5a,b). A regression with all three parameters (R, B5, and $Q(O_{ortho})$) gave a correlation of calculated and observed pK_i values with a r^2 of 0.946 (Figure 5c).

Discussion

Progress in the evaluation of the physiological role of P2 receptors has been impeded by the lack of subtype-selective and potent ligands. Even though suramin is an unspecific compound interacting with an array of P2 receptors,[11,31] this polysulfonated naphthylurea (Figure 1) was very successful as chemical lead in the development of P2 receptor ligands. Taking suramin as chemical lead, our group has contributed to the P2 receptor community a series of P2X-selective ligands some of which are highly potent (NF023, NF279, NF449, NF864).[13,14,16,17,32,33] Among P2Y receptors, suramin shows a small preference for $P2Y_{11}$ receptors[10,12] and is

Table 4. Physicochemical Parameters for Multiple Linear Regression Analysis[a]

compound	substituent	R	B5	$Q(O_{ortho})$
8a	H	0.000	1.00	−0.5049
8b, suramin	CH_3	−0.130	2.04	−0.5035
8c	C_2H_5	−0.100	3.17	−0.5033
8d	isopropyl	−0.100	3.17	−0.5040
8e	phenyl	−0.080	3.11	−0.5100
8f	F	−0.340	1.35	−0.5069
8g	Cl	−0.150	1.80	−0.5032
8h	OCH_3	−0.510	3.07	−0.5107
8i	CH_2OCH_3	0.020	3.40	−0.5014

[a] R: Resonance. B5: size. $Q(O_{ortho})$: partial charge of amide bond oxygen in ortho position of substituents.

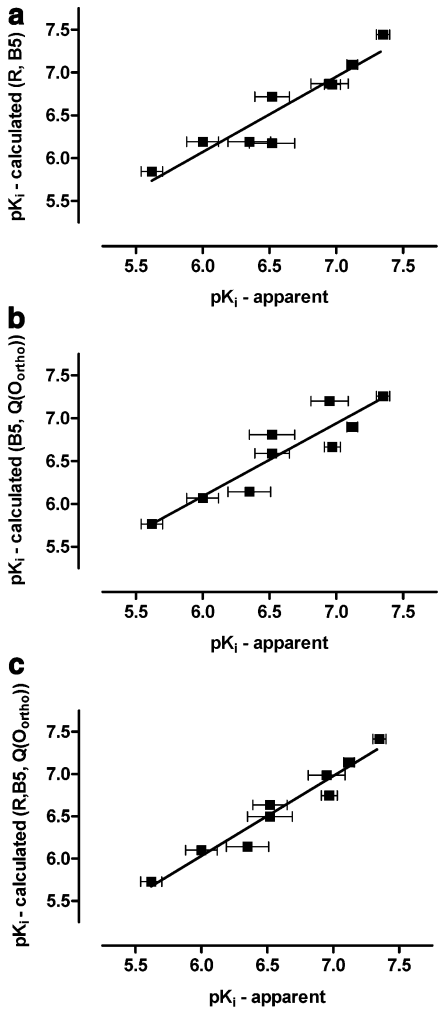

Figure 5. Correlation of estimated apparent pK_i with calculated pK_i values. For pK_i calculations, the following parameters were used: (a) Resonance (R) and size (B5). $pK_i = 7.282 - 2.100R - 0.410B5$. $r^2 = 0.880$. RMSE = 0.182. (b) Size (B5) and partial charge of the ortho oxygen ($Q(O_{ortho})$). $pK_i = -46.066 - 0.443B5 - 106.376Q(O_{ortho})$. $r^2 = 0.851$. RMSE = 0.328. (c) Resonance (R), size (B5), and partial charge of the ortho oxygen ($Q(O_{ortho})$). $pK_i = -22.65 - 1.352R - 0.426B5 - 59.535Q(O_{ortho})$. $r^2 = 0.946$. RMSE = 0.122.

to our knowledge the only known $P2Y_{11}$ receptor antagonist. $P2Y_{11}$ receptors are assumed to be involved in the modulation of the immune system by fostering the maturation of neutrophils and dendritic cells[8,9] and seem to play a role in cardiomyocyte function,[7] but data on the detailed function and physiology of $P2Y_{11}$ receptors remain poor. We thus launched a medicinal chemistry project aiming at the development of $P2Y_{11}$ ligands with increased potency and selectivity compared to suramin. The large ureas **8g**−**i** as suramin analogues and the corresponding nitro and amino precursors were synthesized (Scheme 1). Compounds **3a**−**f**, **4a**−**f**, **5a**−**f**, **6a**−**f**, **7a**−**f**, **8a**, and **8c**−**f** were also prepared as reported by Nickel et al. and Kassack et al.[16,18] All compounds **3**−**8a**−**i** were functionally evaluated (calcium fluorescence)[30] at recombinant $P2Y_{11}$ receptors and at natively expressed $P2Y_1$ and $P2Y_2$ in HEK293 wild-type cells (Tables 1 and 2; data not shown for precursors **3**, **4**, **6**, **7a**−**i** due to their inactivity at $P2Y_1$, $P2Y_2$, and $P2Y_{11}$ up to 100 μM). $P2Y_1$ (stimulation by adenine nucleotides) and $P2Y_2$ (stimulation by uracil nucleotides) represent two major classes of P2Y receptors and were thus chosen for testing on selectivity for $P2Y_{11}$ over other P2Y receptors. The fluorine analogue **8f** of suramin turned out as the most potent $P2Y_{11}$ antagonist in this study (K_i: 44.3 nM) and was ~7-fold more potent than suramin with an at least 650-fold selectivity for $P2Y_{11}$ over $P2Y_1$ and $P2Y_2$ (Figure 3). Tests on the selectivity of **8f** against P2X receptors revealed 3-fold to >67-fold selectivity for $P2Y_{11}$ over $P2X_{2,3,4,7}$ depending on the receptor subtype and showed approximate equipotency at $P2X_1$ and $P2Y_{11}$ receptors (Tables 2 and 3). Whereas **8f** is thus clearly an advance over suramin in both potency and selectivity at $P2Y_{11}$ receptors, **8f** still needs further improvement to also obtain selectivity for $P2Y_{11}$ over the widespread $P2X_1$ receptor.

Reducing the size and thus the distance between the two naphthalene trisulfonic acid residues yielded inactive or very weak (**5b**: K_i: 7.6 μM) small ureas (Tables 1 and 2). Among the large ureas, 53-fold difference in potency between the best compound (**8f**, K_i: 44.3 nM) and the weakest (**8i**, K_i: 2.4 μM) was observed. Since the suramin molecule has been varied in only one position (methyl groups), and obtained compounds showed a 53-fold difference in $P2Y_{11}$ receptor blockade, a Hansch-type QSAR analysis was performed. Best correlations of calculated versus observed biological activity were obtained by regressions with parameters for resonance, size (B5), and partial charges of the amide group oxygen in ortho-position of the residue R ($Q(O_{ortho})$) (Figure 5). Results indicate that an electron-withdrawing residue R (e.g., fluorine, chlorine) has a positive influence on the inhibitory potency whereas large substituents (e.g., ethyl, isopropyl, phenyl, methoxymethyl) lead to a decrease in the inhibition of $P2Y_{11}$ receptors. These correlations are currently being used to predict the potency of further compounds which will then be synthesized.

All nitro and amino precursors were basically inactive at $P2Y_{11}$ (and $P2Y_{1,2}$) receptors up to a concentration of 100 μM (data not shown). A requirement for $P2Y_{11}$ blockade among suramin analogues seems thus a symmetrical molecule with two centers of anionic charges (here: sulfonic acid residues) in a distinct distance. This is consistent with results previously obtained at $P2X_1$ receptors where all asymmetric precursors of NF449, a symmetric highly potent $P2X_1$ antagonist, were inactive at 10−100 μM.[16] Besides the requirements of distinct anionic charges, specific aromatic substitutions of the benzene residues of suramin can lead to large differences in the potency of compounds as seen, e.g., by the 53-fold difference in the potency of the fluorine derivative **8f** and the methoxymethyl derivative **8i** at $P2Y_{11}$ (Table 2). The nature of the interaction of the compounds described in this paper was shown to be competitive as examplified for **8f** (Schild analysis, Figure 4). The pA_2 of **8f** from Schild analysis (7.77, Figure 4) was in accordance with the pK_i from inhibition curves (7.35, Table 2). Suramin has a broad range of side effects at concentrations used to block $P2Y_{11}$ receptor activity.[34] The fact that nanomolar concentrations of the suramin-like compound **8f** are sufficient to antagonize $P2Y_{11}$ receptors effectively and selectively against $P2Y_{1,2}$ and $P2X_{2,3,4,7}$ receptors may allow in vivo studies of the $P2Y_{11}$ receptor physiology without limitations due to toxic side effects occurring with suramin. To achieve selectivity against $P2X_1$ receptors, further modifications of **8f** are necessary.

Conclusion

This study presents the synthesis and structure−activity relationships of a series of suramin analogues and led to the discovery of the first nanomolar potency $P2Y_{11}$ receptor antagonist **8f** with at least 650-fold selectivity for $P2Y_{11}$ over $P2Y_1$ and $P2Y_2$, and a 3- to >67-fold selectivity over $P2X_{2,3,4,7}$ receptors. **8f** is, however, approximately equipotent at $P2Y_{11}$ and $P2X_1$ receptors. A symmetric structure linking two anionic clusters seems to be required for bioactivity. QSAR studies reveal that a substitution with favored values for resonance (R), size (B5), and partial charges of the amide group oxygen in ortho-position of the residue R ($Q(O_{ortho})$) in the aromatic linker region can indeed lead to an increased potency as is the case for the fluorine derivative **8f**. The QSAR results may guide the directed synthesis and development of further potent and selective (also against $P2X_1$) $P2Y_{11}$ ligands. Thus, this study and the novel ligand **8f** may be helpful to obtain a deeper insight into the physiological and pathophysiological role of $P2Y_{11}$ receptors.

Experimental Section

Chemical Synthesis. Suramin and 8-aminonaphthalene-1,3,5-trisulfonic acid disodium salt were gifts from Bayer AG (Leverkusen, Germany). All other reagents were purchased from Fluka, Aldrich, or Sigma (all: Taufkirchen, Germany).

^{1}H NMR spectra were measured on a Varian T 60 (60 MHz), a Varian XL 300 (300 MHz), or a Bruker DRX 500 (500 MHz) spectrometer (Karlsruhe, Darmstadt, Germany) using DMSO-d_6 as a solvent and D_2O for H−D exchange. ^{13}C NMR spectra were recorded on a Varian XL 300 (75 MHz) spectrometer using DMSO-d_6 as a solvent. NMR chemical shifts are reported as δ values (ppm) downfield relative to Me_4Si which was used as internal standard (0 ppm). The following abbreviations are used: s (singlet), d (doublet), dd (double of doublet), dq (double of quartet), dt (double of triplet), pt (pseudotriplet), q (quartet), sep (septet), m (multiplet), ar (aromatic), br (broad), ex (exchangeable with D_2O), J (coupling constant in hertz). IR spectra were recorded with a Perkin-Elmer Spectrophotometer 297 or a FT-IR spectrophotometer "Paragon 1000" from Perkin-Elmer (Rodgau, Germany). Purity of compounds was checked

using a previously published HPLC method.[26] Briefly, a Hewlett-Packard 1050 series HPLC apparatus equipped with a Hewlett-Packard MOS−Hypersil RP-C8 analytical column (5 μM, 100 mm × 2.1 mm) and a Hewlett-Packard MOS-Hypersil RP−C8 as precolumn (5 μM, 20 mm × 2.1 mm) were used. Temperature of the column was kept at 37 °C. The gradient solvent system consisted of a mixture of 6.25 mM tetrabutylammonium hydrogensulfate in 0.02 M phosphate buffer pH 6.5 and methanol starting at 80:20. A linear gradient was applied reaching a mixture of 46:54 within 8 min. The flow rate was retained at 0.6 mL/min. Peaks were detected by UV absorption using a Hewlett-Packard 1040A diode array detector. All compounds tested for biological activity showed ≥95% purity in the HPLC analysis. Thin-layer chromatography (TLC) was performed with all compounds on 20 × 20 cm aluminum sheets precoated with silica gel 60 F_{254} from Merck (Darmstadt, Germany). Elution solvent mixture was toluene:acetone:formic acid = 6:3.9:0.1 (EM1), dioxane:ammonia (25%) = 8:2 (EM2), 2-propanol:ammonia (25%) = 5:2 (EM3), or dioxane:water:glacial acetic acid = 7.5:1.5:1 (EM4). TLC confirmed ≥95% purity for all compounds. Low-resolution ES (electron spray) mass spectrometry was carried out on a API2000 Applied Biosystems/MDS SCIEX LC/MS mass spectrometer from Applied Biosystems (Darmstadt, Germany). Solvent for the measurement was a mixture of 2 mM ammonium acetate in water and 2 mM ammonium acetate in methanol (1:1; pH 7). Melting points were measured with a FP 61 apparatus from Mettler (Giessen, Germany). Melting points of the sulfonic acid derivatives were greater than 300 °C. Sodium chloride content was estimated by potentiometric titration analysis on a titroprocessor 672 from Metrohm (Herisau, Switzerland) and found to be between 0.6 and 79.4%. The synthesized sulfonic acid derivatives contain crystal water which was estimated by Karl Fischer titration analysis using a Titrino 701 KT from Metrohm (Herisau, Switzerland). Between 2.5 and 19.5 mol H_2O per mol of compound were found. Elemental analyses (C, H, N) were performed on a Perkin-Elmer Elementaranalysator 240 B (Rodgau, Germany) or a Vario EL apparatus from Elementar (Hanau, Germany). After subtraction of the sodium chloride and water content, elemental analyses data were evaluated and found to be within ±0.4%.

Pharmacological Experiments. Cell Culture and Measurements of Intracellular Calcium. All methods have been previously described in detail.[16,30] HEK293 cells were grown in Dulbecco's modified Eagle Medium Nutrient Mixture F-12 Ham (DMEM/F12 1:1 Mixture) (Sigma-Aldrich) containing 100 U/mL penicillin G, 100 μg/mL streptomycin, 10% fetal bovine serum, and 5 mM L-glutamine (Sigma-Aldrich). 1321N1-$P2Y_{11}$ astrocytoma cells stably transfected with a plasmid containing the human $P2Y_{11}$ coding sequence (AF030335)[27] were cultured in Dulbecco's modified Eagle Medium (DMEM) with glutamax-I, sodium pyruvate, glucose (4500 mg/L), and pyridoxine (Gibco) supplemented with 100 U/mL penicillin G, 100 μg/mL streptomycin, 10% fetal bovine serum, and 200 μg/mL G418 (Sigma-Aldrich). Cells were incubated at 37 °C in 5% CO_2.

Ca^{2+} fluorescence was measured as previously described using a fluorescence microplate reader with a pipettor system (NOVOstar; BMG LabTech, Offenburg, Germany).[30] Harvested cells (0.05% trypsin/0.02% EDTA, Sigma Aldrich) were rinsed with the appropriate culture medium. After centrifugation, the pelleted cells were resuspended in fresh medium and kept at 37 °C under 5% CO_2 for 20 min. After washing two times with Krebs-HEPES buffer, cells were loaded with Oregon Green 488 BAPTA-1/AM (3 μM; Molecular Probes, Eugene, OR) for 60 min at 25 °C in the same buffer containing 1% Pluronic F-127 (Sigma-Aldrich). After rinsing three times with Krebs-HEPES buffer, the cell suspension was diluted and evenly plated into 96-well plates (Greiner, Frickenhausen, Germany) at a density of 50−100 000 cells/well. Concentration−response curves of agonists were obtained by injection of increasing concentrations of 2-MeSADP (native $P2Y_1$ receptors in HEK293 cells) or UTP (native $P2Y_2$ receptors in HEK293 cells) or ATPγS (1321N1-$P2Y_{11}$ cells). Excitation wavelength was 485 nm (bandwidth 12 nm), and fluorescence intensity was monitored at 520 nm (bandwidth 35 nm) for 30 s at 0.4 s intervals. Concentration−inhibition curves of antagonists were obtained by preincubating the cells with test compounds for 30 min at 37 °C and subsequent injection of agonist (31.6 nM 2-MeSADP, 3.16 μM UTP, or 1 μM ATPγS, respectively).

Electrophysiological Evaluation of 8f at Recombinant P2X Receptors. The inhibitory potency of **8f** at P2X receptors was evaluated on *X. laevis* oocytes recombinantly expressing various rat (r) and human (h) P2X subtypes ($rP2X_1$, $hP2X_1$, rPX_2, $rP2X_3$, $hP2X_3$, $rP2X_4$, $hP2X_4$, $rP2X_7$) using previously described protocols.[17,35] Concentration−inhibition curves and IC_{50} values were derived from nonlinear least-squares fits of the Hill equation to the pooled data. The nondesensitizing properties of the $rP2X_2$ receptor allowed quantifying inward current inhibition under steady-state conditions by coapplying **8f** during continued stimulation with ATP. Current inhibition occurred almost instantaneously as inferred from the immediate decrease of the current amplitude upon coapplication of an effective **8f** concentration. The classical Cheng−Prusoff equation could be applied to calculate the K_i value of **8f** for the $rP2X_2$ receptor. The inhibitory potency of **8f** at desensitizing P2X receptors was determined from peak current measurements. As detailed previously, an accurate assessment of IC_{50} values for desensitizing receptors can usually not be achieved by coapplying agonist and antagonist, as the agonist-induced current will start to decline by desensitization before a binding equilibrium between the two compounds is reached. To account for this problem, oocytes expressing desensitizing P2X receptors were preequilibrated with **8f** for 15 s before being challenged with ATP in the continued presence of **8f**. We have previously shown that suramin derivatives block P2X receptors competitively.[35,36] Accordingly, if **8f** does not dissociate significantly from the receptor during the time needed to reach the peak current response, ATP can only bind to receptors unoccupied by **8f**, leading to a pseudo-irreversible type of inhibition. Under these conditions, K_i and IC_{50} values will be equal. We therefore assume that the IC_{50} values deduced from peak current measurements are close or equal to the K_i values. In any case, K_i values deviate from IC_{50} values maximally by a factor of 2, as ATP was applied at a concentration close to its EC_{50} value. All results are presented as means ± SEM from at least three experiments.

Reverse-Transcriptase Polymerase Chain Reaction (RT-PCR). Total RNA from HEK293 cells was isolated with TRI-reagent (Sigma, Taufkirchen, Germany) according to the manufacturer's instructions. Reverse transcription was performed with Enhanced Avian HS RT-PCR Kit (HSRT-100, Sigma) according to the manufacturer's instructions. PCR amplification of $P2Y_1$ or $P2Y_2$ receptor-specific fragments was performed with the following primer pairs (Operon Biotechnologies, Cologne, Germany): $P2Y_1$ forward primer: 5′-TTACGACACCACCTCAGACG-3′. $P2Y_1$ reverse primer: 5′-TGAAAGTATCTCCCGCCAAG-3′ (389bp PCR product); $P2Y_2$ forward primer: 5′-AGTGGTCTGGAATGGACTGG-3′. $P2Y_2$ reverse primer: 5′-TTGGAGAAAGGACCCTTGTG-3′ (247bp PCR product). The PCR mixture contained in a total volume of 20 μL or 10 μL of PCR Mastermix (Bio-Rad, Munich, Germany), PCR forward and reverse primers in a final concentration of 500 nM, and 1.5 μL of the RT-product (first strand cDNA). PCR amplifications were performed on a DNA Engine Opticon (MJ research, Waltham, MA). Reaction conditions for the PCR were 40 cycles with 20 s at 94 °C, 30 s at 59 °C, and 60 s at 72 °C. Reaction products were analyzed by electrophoresis on a 2% agarose gel.

QSAR Analysis. Fragment constant descriptors for physicochemical properties were derived from BuildQSAR (University of Espirito Santo, Brazil).[37] For each homologue, one-half of the symmetric molecule, abandoning the naphthalene sulfonic acid residues, was built using SYBYL 7.0 (Tripos Inc., St.Louis, MO). Geometrical optimization and calculation of Mulliken partial charges of the amide group in ortho-position of the residue R were performed with the hybrid DFT method

B3LYP and basis set 6-31G (d,p), using the Gaussian03 software package (Gaussian Inc., Pittsburgh, PA). Using these parameters, a multiple linear regression analysis was conducted using MOE 2004.03 (Chemical Computing Group Inc., Montreal, Canada).

Data Analysis of Intracellular Calcium Measurements. Effects of single doses of antagonists (100 μM) were expressed as a percentage of the agonist control responses. Antagonist IC_{50} values ($pIC_{50} = -\log IC_{50}$) represent the concentration needed to inhibit by 50% the effect elicited by single doses of agonists. Apparent functional K_i values ($pK_i = -\log K_i$) were calculated according to the equation of Cheng and Prusoff:[38]

$$K_i = IC_{50}/(1 + L/EC_{50})$$

where IC_{50} is the inhibitory concentration 50% of the antagonist, EC_{50} is the effective concentration 50% of the used agonist, and L is the molar concentration of the used agonist. IC_{50} values for antagonists and EC_{50} values for agonists were derived from −log concentration − effect (inhibition) curves fitted to the pooled data by logistic, nonlinear regression analysis (Prism 4.00, GraphPad Software, San Diego, CA).

Acknowledgment. This work was supported by DFG (Deutsche Forschungsgemeinschaft) grants GRK677/1 and GRK677/2 to H.U. and M.U.K. and FOR450 (TP11) to G.S., and by the START program of the Faculty of Medicine, RWTH Aachen University, to R.H. S.M. was supported by a stipend provided by the Bischöfliche Studienförderung Cusanuswerk. D.H. was supported by a stipend from the DAAD (Deutscher Akademischer Austauschdienst). We further acknowledge the assistance of Mrs. M. Schneider for measuring the mass spectra.

Appendix

Abbreviations: ATPγS: adenosine-5′-*O*-(3-thiotriphosphate); cAMP: cyclic 3′,5′-adenosinemonophosphate; 2-MeSADP: 2-methylthio-adenosine-5′-diphosphate; PPADS: pyridoxal-5′-phosphate-6-azophenyl-2′,4′-disulfonic acid; SEM: standard error of the mean.

Supporting Information Available: Synthetic procedures and compound monographs (analytical data). This material is available free of charge via the Internet at http://pubs.acs.org.

References

(1) Burnstock, G. A basis for distinguishing two types of purinergic receptor. In *Cell membrane receptors for* drugs and hormones: a multidisciplinary approach; Straub, R. W., Bolis, L. Eds.; Raven Press: New York, 1978; pp 107−118.
(2) Khakh, B. S.; Burnstock, G.; Kennedy, C.; King, B. F.; North, R. A.; Seguela, P.; Voigt, M.; Humphrey, P. P. International union of pharmacology. XXIV. Current status of the nomenclature and properties of P2X receptors and their subunits. *Pharmacol. Rev.* **2001**, *53*, 107−118.
(3) Abbracchio, M. P.; Boeynaems, J. M.; Barnard, E. A.; Boyer, J. L.; Kennedy, C.; Miras-Portugal, M. T.; King, B. F.; Gachet, C.; Jacobson, K. A.; Weisman, G. A.; Burnstock, G. Characterization of the UDP-glucose receptor (re-named here the P2Y14 receptor) adds diversity to the P2Y receptor family. *Trends Pharmacol. Sci.* **2003**, *24*, 52−55.
(4) Muller, C. E. P2-pyrimidinergic receptors and their ligands. *Curr. Pharm. Des.* **2002**, *8*, 2353−2369.
(5) Zhang, F. L.; Luo, L.; Gustafson, E.; Palmer, K.; Qiao, X.; Fan, X.; Yang, S.; Laz, T. M.; Bayne, M.; Monsma, F., Jr. P2Y(13): identification and characterization of a novel Galphai-coupled ADP receptor from human and mouse. *J. Pharmacol. Exp. Ther.* **2002**, *301*, 705−713.
(6) Jacobson, K. A.; King, B. F.; Burnstock, G. Pharmacological characterization of P2 (nucleotide) receptors. *Celltransmissions* **2000**, *16*, 3−16.
(7) Balogh, J.; Wihlborg, A. K.; Isackson, H.; Joshi, B. V.; Jacobson, K. A.; Arner, A.; Erlinge, D. Phospholipase C and cAMP-dependent positive inotropic effects of ATP in mouse cardiomyocytes via P2Y(11)-like receptors. *J. Mol. Cell Cardiol.* **2005**, *39*, 223−230.
(8) van der Weyden, L.; Conigrave, A. D.; Morris, M. B. Signal transduction and white cell maturation via extracellular ATP and the P2Y11 receptor. *Immunol. Cell Biol.* **2000**, *78*, 369−374.
(9) Wilkin, F.; Duhant, X.; Bruyns, C.; Suarez-Huerta, N.; Boeynaems, J. M.; Robaye, B. The P2Y11 receptor mediates the ATP-induced maturation of human monocyte-derived dendritic cells. *J. Immunol.* **2001**, *166*, 7172−7177.
(10) Communi, D.; Robaye, B.; Boeynaems, J. M. Pharmacological characterization of the human P2Y11 receptor. *Br. J. Pharmacol.* **1999**, *128*, 1199−1206.
(11) Dunn, P. M.; Blakeley, A. G. Suramin: a reversible P2-purinoceptor antagonist in the mouse vas deferens. *Br. J. Pharmacol.* **1988**, *93*, 243−245.
(12) Jacobson, K. A.; Jarvis, M. F.; Williams, M. Purine and pyrimidine (P2) receptors as drug targets. *J. Med. Chem.* **2002**, *45*, 4057−4093.
(13) Damer, S.; Niebel, B.; Czeche, S.; Nickel, P.; Ardanuy, U.; Schmalzing, G.; Rettinger, J.; Mutschler, E.; Lambrecht, G. NF279: a novel potent and selective antagonist of P2X receptor-mediated responses. *Eur. J. Pharmacol.* **1998**, *350*, R5−R6.
(14) Soto, F.; Lambrecht, G.; Nickel, P.; Stuhmer, W.; Busch, A. E. Antagonistic properties of the suramin analogue NF023 at heterologously expressed P2X receptors. *Neuropharmacology* **1999**, *38*, 141−149.
(15) Hülsmann, M.; Nickel, P.; Kassack, M.; Schmalzing, G.; Lambrecht, G.; Markwardt, F. NF449, a novel picomolar potency antagonist at human $P2X_1$ receptors. *Eur. J. Pharmacol.* **2003**, *470*, 1−7.
(16) Kassack, M. U.; Braun, K.; Ganso, M.; Ullmann, H.; Nickel, P.; Boing, B.; Muller, G.; Lambrecht, G. Structure−activity relationships of analogues of NF449 confirm NF449 as the most potent and selective known $P2X_1$ receptor antagonist. *Eur. J Med. Chem.* **2004**, *39*, 345−357.
(17) Rettinger, J.; Braun, K.; Hochmann, H.; Kassack, M. U.; Ullmann, H.; Nickel, P.; Schmalzing, G.; Lambrecht, G. Profiling at recombinant homomeric and heteromeric rat P2X receptors identifies the suramin analogue NF449 as a highly potent P2X-(1) receptor antagonist. *Neuropharmacology* **2005**, *48*, 461−468.
(18) Nickel, P.; Haack, H. J.; Widjaja, H.; Ardanuy, U.; Gurgel, C.; Duwel, D.; Loewe, H.; Raether, W. Potential filaricides. Suramin analogs. *Arzneimittelforschung.* **1986**, *36*, 1153−1157.
(19) Corson, B. B.; Hazen, R. K. *Organic Synthesis*; Wiley: New York, 1943; pp 434−438.
(20) Harwood: L. M.; Moody, C. J.; Percy, J. M. *Experimental Organic Chemistry: Standard and* Microscale; Blackwell Science (UK): Oxford, 1999.
(21) Olson, E. S. A modification of the free radical bromination of p-toluic acid. *J. Chem. Educ.* **1980**, *57*, 157.
(22) Gattermann, L.; Wieland, H. *Die Praxis des organischen Chemikers; Carbonsäurechloride und Säureanhydride*; Walter de Gruyter: Berlin; New York, 1982; p 304.
(23) Henecka, H. *Methoden der Organischen Chemie: Carbonsäurechloride aus Carbonsäuren/Einwirkung von Thionylchlorid auf Carbonsäuren (Houben-Weyl)*; Georg Thieme Verlag: Stuttgart, 1952; pp 610−612.
(24) Muth, H.; Sauerbier, M. *Methoden der Organischen Chemie: Reduktion (Houben-Weyl)*; Georg Thieme Verlag: Stuttgart, 1980; pp 645−654.
(25) Kreimeyer, A.; Muller, G.; Kassack, M.; Nickel, P.; Gagliardi, A. R. Suramin analogues with a 2-phenylbenzimidazole moiety as partial structure; potential anti HIV- and angiostatic drugs, 2: Sulfanilic acid-, benzenedisulfonic acid-, and naphthalenetrisulfonic acid analogues. *Arch. Pharm. (Weinheim)* **1998**, *331*, 97−103.
(26) Kassack, M.; Nickel, P. Rapid, highly sensitive gradient narrow-bore high-performance liquid chromatographic determination of suramin and its analogues. *J. Chromatogr. B Biomed. Appl.* **1996**, *686*, 275−284.
(27) Communi, D.; Govaerts, C.; Parmentier, M.; Boeynaems, J. M. Cloning of a human purinergic P2Y receptor coupled to phospholipase C and adenylyl cyclase. *J. Biol. Chem.* **1997**, *272*, 31969−31973.
(28) Schachter, J. B.; Sromek, S. M.; Nicholas, R. A.; Harden, T. K. HEK293 human embryonic kidney cells endogenously express the P2Y1 and P2Y2 receptors. *Neuropharmacology* **1997**, *36*, 1181−1187.
(29) Yu, H.; Bianchi, B.; Metzger, R.; Lynch, K.; Kowaluk, E.; Jarvis, M. F.; Van Biesen, T. Lack of specificity of [35S]-ATPgammaS and [35S]-ADPbetaS as radioligands for ionotropic and metabotropic P2 receptor binding. *Drug Dev. Res.* **2005**, *48*, 84−93.

(30) Kassack, M. U.; Hofgen, B.; Lehmann, J.; Eckstein, N.; Quillan, J. M.; Sadee, W. Functional Screening of G Protein-Coupled Receptors by Measuring Intracellular Calcium with a Fluorescence Microplate Reader. *J. Biomol. Screen.* **2002**, *7*, 233−246.
(31) Charlton, S. J.; Brown, C. A.; Weisman, G. A.; Turner, J. T.; Erb, L.; Boarder, M. R. PPADS and suramin as antagonists at cloned P2Y- and P2U-purinoceptors. *Br. J. Pharmacol.* **1996**, *118*, 704−710.
(32) Hechler, B.; Magnenat, S.; Zighetti, M. L.; Kassack, M. U.; Ullmann, H.; Cazenave, J. P.; Evans, R.; Cattaneo, M.; Gachet, C. Inhibition of platelet functions and thrombosis through selective or nonselective inhibition of the platelet P2 receptors with increasing doses of NF449 [4,4′,4″,4‴-(carbonylbis(imino-5,1,3-benzenetriylbis-(carbonylimino)))t etrakis-benzene-1,3-disulfonic acid octasodium salt]. *J Pharmacol. Exp. Ther.* **2005**, *314*, 232−243.
(33) Lambrecht, G.; Braun, K.; Damer, M.; Ganso, M.; Hildebrandt, C.; Ullmann, H.; Kassack, M. U.; Nickel, P. Structure−activity relationships of suramin and pyridoxal-5′-phosphate derivatives as P2 receptor antagonists. *Curr. Pharm. Des.* **2002**, *8*, 2371−2399.
(34) Voogd, T. E.; Vansterkenburg, E. L.; Wilting, J.; Janssen, L. H. Recent research on the biological activity of suramin. *Pharmacol. Rev.* **1993**, *45*, 177−203.
(35) Rettinger, J.; Schmalzing, G.; Damer, S.; Muller, G.; Nickel, P.; Lambrecht, G. The suramin analogue NF279 is a novel and potent antagonist selective for the P2X(1) receptor. *Neuropharmacology* **2000**, *39*, 2044−2053.
(36) Rettinger, J.; Schmalzing, G. Desensitization masks nanomolar potency of ATP for the $P2X_1$ receptor. *J Biol. Chem.* **2004**, *279*, 6426−6433.
(37) Oliveira, D. B.; Gaudio, A. C. BuildQSAR: A New Computer Program for QSAR Analysis. *Quant. Struct.-Act. Relat.* **2000**, *19*, 599−601.
(38) Cheng, Y.; Prusoff, W. H. Relationship between the inhibition constant (Ki) and the concentration of inhibitor which causes 50% inhibition (IC50) of an enzymatic reaction. *Biochem. Pharmacol.* **1973**, *22*, 3099−3108.
(39) Fahim, H. A.; Fleifel, A. M. The preparation of some 4-*n*-alkyl-3-nitrobenzoic acids. *J. Chem. Soc.* **1952**, 4519−4521.
(40) Bryan, J. T.; Foote, P. A. Synthesis of local anesthetics derived from cumic and 3-nitrocumic acids. *J. Am. Pharm. Assoc.* **1950**, *39*, 644−655.
(41) Grieve, W. S. M.; Hey, D. H. Substitution in compounds containing two or more phenyl groups. Part I. The nitration of 4-methyldiphenyl. *J. Chem. Soc.* **1932**, 1888−1894.
(42) Sala, T.; Sargent, M. V. Tetrabutylammonium permanganate: an efficient oxidant for organic substrates. *J. Chem. Soc., Chem. Commun.* **1978**, 253−254.

JM050301P